Theory of $d^{10}-d^{10}$ Closed-Shell Attraction. III. Rings

Pekka Pyykkö* and Fernando Mendizabal†

Department of Chemistry, University of Helsinki, P.O.B. 55 (A.I. Virtasen aukio 1), FIN-00014 Helsinki, Finland

Received January 30, 1998

We study the dependence of the intramolecular M^I-M^I interaction on electron correlation effects in eight-membered rings of type $[M_2(PH_2CH_2PH_2)_2]^{2+}$, $[M_2(NHCHNH)_2]$, $[M_2(SCHS)_2]$ (M = Au, Ag, Cu), $[Au_2(PH_2CH_2PH_2)_2]Cl_2$, halogenometal(I) $[M_2X_4]^{2-}$ (M = Au, Ag, Cu; X = Cl, Br, I), and $[Au_2Te_4]^{2-}$ at the quasirelativistic pseudopotential ab initio MP2 and Hartree−Fock levels. The intramolecular M^I-M^I distances, *R*, at the MP2 level fall in the same range as the experimental ones. The *R* values are reduced from HF to MP2 level. All the calculations suggest that correlation effects are essential. The reduction of *R* depends on the particular M−L combination (L = ligand). In the rings, short Cu^I-Cu^I distances are recovered for the first time. The explicit inclusion of the counterions is unimportant for M^I and essential for M^{II}, as shown by a study of the oxidative addition of Cl_2 to the model $[Au_2(CH_2PH_2CH_2)_2]$. The Au(I) is then oxidized to Au(II), and the Au−Au distance is shortened to 261 pm, corresponding to a σ bond. This value is in agreement with experiment.

I. Introduction

It is now well established that attractive intra- and intermolecular secondary bonding interactions between d^{10} cations lead to formation of dimers, oligomers, chains, and sheets.[1−3] At the theoretical level, correlation effects are necessary to obtain any attraction and relativistic effects are partially responsible for its strength.[4−8] The technical requirements for such calculations are described in Parts I and II.[7,8]

NMR experiments allow an estimate of the secondary bond strength and have given values of 29−46 kJ/mol for each Au^I-Au^I bond. Recent optical measurements of the dimerization energies of two eight-membered rings to a ring dimer gave even higher ΔH (Au···Au) values.[9] This interaction is an order of magnitude stronger than the van der Waals attraction in Xe_2, for instance, and of the same order as the strength of typical hydrogen bonds.[10−12]

For the case of the intramolecular interactions, the presence of a bridging ligand should facilitate intramolecular metal(I)−metal(I) contacts in di- or polynuclear complexes. Examples on short M^I-M^I distances exist for the three coinage metals.[1−3,13−16] We have considered the singly bridged, A-frame systems before.[5]

Chart 1

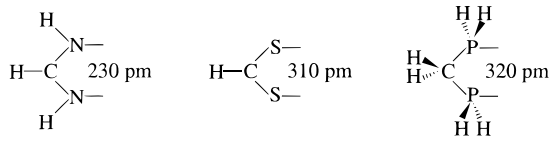

1 **2** **3**

Why are ring systems important? In Parts I and II of this paper[7,8] we have studied the metallophilic attraction in free dimers, without steric constraints from bridging ligands. In the present ring systems the M−M interaction has to compete against the preferences of the ligand. This paper is the first study of such ring systems using correlated ab initio methods and basis sets of the present size.

Of the present ligands, −NH(CH)NH−, **1**, is "hard" and has a short bite distance of 230 pm. The −S(CH)S−, **2**, and $-PH_2CH_2PH_2-$, **3**, ligands are "soft" and have large bite distances of 310 and 320 pm, respectively. Experimentally, systems containing ligands of the type **1** are known for Cu and Ag while systems with ligands of the types **2** and **3** are known for Ag and Au (Chart 1). More generally, these eight-membered rings can have a structure $[M_2(XZX)_2]$, M = Au, Ag, Cu; X = PR_2, NR, S; Z = PR_2, CR_2, NR (R = $-CH_3$, $-C_6H_5$) (see Figure 1).[17,18,20−24] Furthermore, the two X groups can be different (X and Y).

* Fax: 358-9-191 40169. E-mail: Pekka.Pyykko@helsinki.fi.
† Present and permanent address: Department of Chemistry, Faculty of Science, University of Chile.

(1) Schmidbaur, H. *Gold Bull.* **1990**, *23*, 11.
(2) Schmidbaur, H. *Chem. Soc. Rev.* **1995**, 391.
(3) Pyykkö, P. *Chem. Rev.* **1997**, *97*, 597.
(4) Pyykkö, P.; Zhao, Y.-F. *Angew. Chem.* **1991**, *103*, 622; *Angew. Chem., Int. Ed. Engl.* **1991**, *30*, 604.
(5) Li, J.; Pyykkö, P. *Chem. Phys. Lett.* **1992**, *197*, 586.
(6) Pyykkö, P.; Li, J.; Runeberg, N. *Chem. Phys. Lett.* **1994**, *218*, 133.
(7) Pyykkö, P.; Runeberg, N.; Mendizabal, F. *Chem. Eur. J.* **1997**, *3*, 1451.
(8) Pyykkö, P.; Mendizabal, F. *Chem. Eur. J.* **1997**, *3*, 1458.
(9) Tang, S. S.; Chang, C.-P.; Lin, I. J. B.; Liou, L.-S.; Wang, J.-C. *Inorg. Chem.* **1997**, *36*, 2294.
(10) Schmidbaur, H.; Graf, W.; Müller, G. *Angew. Chem., Int. Ed. Engl.* **1988**, *27*, 417.
(11) Narayanaswamy, R.; Young, M. A.; Parkhurst, E.; Ouellette, M.; Kerr, M. E.; Ho, D. M.; Elder, R. C.; Bruce, A. E.; Bruce, M. R. M. *Inorg. Chem.* **1993**, *32*, 2506.
(12) Harwell, D. E.; Mortimer, M. D.; Knobler, C. B.; Anet, F. A. L.; Hawthorne, M. F. *J. Am. Chem. Soc.* **1996**, *118*, 2679.
(13) Wells, A. F. *Structural Inorganic Chemistry*, 5th ed.; Clarendon Press: Oxford, 1984; pp 1104−1107.
(14) Viski, P.; Waller, D. P.; Zuraw, M. *J. Org. Chem.* **1996**, *61*, 7631.
(15) Irwin, M. J.; Rendina, L. M.; Vittal, J. J.; Puddephatt, R. J. *Chem. Commun.* **1996**, 1281.
(16) Warren, C. J.; Ho, D. M.; Bocarsly, A. B.; Haushalter, R. C. *J. Am. Chem. Soc.* **1993**, *115*, 6417.
(17) Cotton, F. A.; Feng, X.; Matusz, M.; Poli, R. *J. Am. Chem. Soc.* **1988**, *110*, 7077.
(18) Hesse, R.; Jennische, P. *Acta Chem. Scand.* **1972**, *26*, 3855.
(19) Ho, D. M.; Bau, R. *Inorg. Chem.* **1983**, *22*, 4073.
(20) Payne, N. C.; Puddephatt, R. J.; Ravindranath, R.; Treurnicht, I. *Can. J. Chem.* **1988**, *66*, 3176.

S0020-1669(98)00121-9 CCC: $15.00
Published on Web 05/23/1998

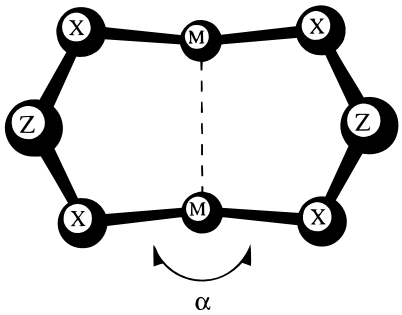

Figure 1. Eight-membered rings and their geometrical variables.

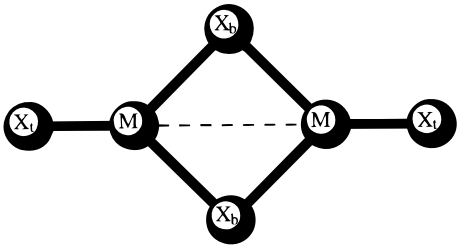

Figure 2. Di-μ -halogenodihalogenometal(I) systems.

The structures can adopt chair, boat, or planar geometries, and they all have two X−M−Y axes (X,Y = ligand) running parallel to each other. In general, for a large number of structures of these eight-membered rings, the transannular Au−Au contacts are found consistently at the distance of 300 ± 25 pm, independently of the ring conformation.[1−3] The X−M−Y axes are often not linear, but they show an angle smaller than 180° in such an orientation that the metal atoms come closer together. This has been used as an indication of the intramolecular attraction. Note that the bending should be inward or outward for $R > R_e$ and $R < R_e$, respectively, where R_e is the free-dimer equilibrium M−M distance, without bridges.

Other types of intramolecular M^I-M^I interaction occur in some halogenocuprates(I) and halogenoargentates(I) of formula $[M_2X_4]^{2-}$ (see Figure 2), with M = Cu, Ag; X = Cl, Br, I. Rather short M^I-M^I distances again occur and suggest a direct "metallophilic" attraction[3] between the M^I cations,[25−29] in contrast to the earlier impression that these structural features encountered in rings and bridged systems could solely be ascribed to the geometry imposed by the ligands and not to any significant M^I-M^I attraction.[30] The first ab initio study of the transannular Au^I-Au^I distance in a $[CH_2(PH_2AuPH_2)_2CH_2]^{2+}$ model at LANL1DZ level showed a dramatic reduction of 52.4 pm from HF to MP2 level.[24] This result shows the importance of electron correlation at the MP2 level for the Au−Au distance, although the ligand geometry remains almost unchanged. However, the calculated Au−Au distance was 347 pm, compared to the experimental value of 297 pm.[20]

In the third part of this study (Parts I and II[7,8]), we investigate the origin and characteristics of the intramolecular M^I-M^I contacts using the eight-membered ring structures of type $[M_2(PH_2CH_2PH_2)_2]^{2+}$, $[M_2(NHCHNH)_2]$, and $[M_2(SCHS)_2]$ (M = Au, Ag, Cu). We also study the possible effect of the counterions on the M^I-M^I distances by explicitly including axial or bridging chlorine atoms in $[Au_2(PH_2CH_2PH_2)_2]Cl_2$ (see Figure 3). Oxidative addition leading to $[(Au^{II})_2(CH_2PH_2CH_2)_2]Cl_2$ is also considered (see Figure 4). Furthermore, we also study the simpler rings $[M_2X_4]^{2-}$ (M = Au, Ag, Cu; X = Cl, Br, I) and $[Au_2Te_4]^{2-}$.

The objective is to study theoretically the intramolecular interaction, comparing each model at the HF and MP2 levels, thus allowing correlation effects on the M^I-M^I distances to be estimated.

II. Computational Details and Theory

The Gaussian 94 package was used.[31] The basis sets and pseudopotentials (PP) used in the production runs are given in Table 1. The 19-valence electron (VE) quasirelativistic (QR) pseudopotential of Andrae[32] and the 11-VE "LANL1DZ" PP[33] were employed for gold. The silver[32] and copper[34] atoms were treated by a 19-VE Stuttgart PP. It was found earlier that two f-type polarization functions for Au, Ag, and Cu are desirable for a correct description of the interaction energy.[7] For gold, their exponents are 0.2 and 1.19. The diffuse one is required for describing the metallophilic attraction and the compact one for describing the covalent bonds. If only one can be afforded, the diffuse one should be taken, as done in our earlier studies.

The atoms C, N, P, S, Te, Cl, Br, and I were also treated by Stuttgart pseudopotentials,[35] including only the valence electrons for each atom. For these atoms, double-zeta basis sets of[35] were used, augmented by d-type polarization functions.[36] For the H atom, a double-zeta plus one p-type polarization function was used[37] (see Table 1).

We have fully optimized the structures assuming a D_{2h} symmetry for the models $[M_2(PH_2CH_2PH_2)_2]^{2+}$, $[Au_2(PH_2CH_2PH_2)_2]Cl_2$, $[M_2(NHCHNH)_2]$, $[M_2(SCHS)_2]$ (M = Au, Ag, Cu), $[M_2X_4]^{2-}$ (M = Au, Ag, Cu; X = Cl, Br, I) and $[Au_2Te_4]^{2-}$ at Hartree−Fock (HF) and MP2 levels. We study the intramolecular interactions using the difference between the M^I-M^I distances and X−M−X angles calculated at HF and MP2 levels as criterion for each model. This gives an idea of the contribution of the electronic correlation to the intramolecular contacts for the ring systems.

III. Results and Discussion

A. Eight-Membered Rings. We have fully optimized the geometries for the eight-membered rings at HF and MP2 levels. A D_{2h} point symmetry was assumed. The XMX angle, α, was defined as the outer one, see Figure 1.

(21) Schmidbaur, H.; Pollok, T. H.; Herr, K.; Wagner, F. E.; Bau, R.; Riede, J.; Müller, G. *Organometallics* **1986**, *5*, 566.
(22) Shain, J.; Fackler, J. P. *Inorg. Chim. Acta* **1987**, *131*, 157.
(23) Perreault, D.; Drouin, M.; Michel, A.; Miskowski, V. M.; Schaefer, W. P.; Harvey, P. D. *Inorg. Chem.* **1992**, *31*, 695.
(24) Fernández, E. J.; Gimeno, M. C.; Jones, P. G.; Laguna, A.; Laguna, M.; López-de-Luzuriaga, J. M.; Rodríguez, M. A. *Chem. Ber.* **1995**, *128*, 121.
(25) Asplund, M.; Jagner, S. *Acta Chem. Scand., Ser. A* **1984**, *38*, 135.
(26) Asplund, M.; Jagner, S. *Acta Chem. Scand., Ser. A* **1984**, *38*, 297.
(27) Helgesson, G.; Jagner, S. *J. Chem. Soc., Dalton Trans.* **1988**, 2117.
(28) Helgesson, G.; Jagner, S. *J. Chem. Soc., Dalton Trans.* **1990**, 2413.
(29) Jagner, S.; Helgesson, G. *Adv. Inorg. Chem.* **1991**, *37*, 1.
(30) Schmidbaur, H.; Wohlleben, A.; Wagner, F.; Orama, O.; Huttner, G. *Chem. Ber.* **1977**, *110*, 1748.
(31) Frisch, M. J.; Trucks, G. W.; Schlegel, H. B.; Gill, P. M. W.; Johnson, B. G.; Robb, M. A.; Cheeseman, J. R.; Keith, T. A.; Petersson, G. A.; Montgomery, J. A.; Raghavachari, K.; Al-Laham, M. A.; Zakrzewski, V. G.; Ortiz, J. V.; Foresman, J. B.; Cioslowski, J.; Stefanov, B. B.; Nanayakkara, A.; Challacombe, M.; Peng, C. Y.; Ayala, P. Y.; Chen, W.; Wong, M. W.; Andres, J. L.; Replogle, E. S.; Gomperts, R.; Martin, R. L.; Fox, D. J.; Binkley, J. S.; Defrees, D. J.; Baker, J.; Stewart, J. P.; Head-Gordon, M.; Gonzalez, C.; Pople, J. A. *Gaussian 94*; Gaussian, Inc.: Pittsburgh, PA, 1995.
(32) Andrae, D.; Häusserman, U.; Dolg, M.; Stoll, H.; Preuss, H. *Theor. Chim. Acta* **1990**, *77*, 123.
(33) Hay, P. J.; Wadt, W. R. *J. Chem. Phys.* **1985**, *82*, 270.
(34) Dolg, M.; Wedig, U.; Stoll, H.; Preuss, H. *J. Chem. Phys.* **1987**, *86*, 866.
(35) Bergner, A.; Dolg, M.; Küchle, W.; Stoll, H.; Preuss, H. *Mol. Phys.* **1993**, *80*, 1431.
(36) Huzinaga, S. *Gaussian Basis Sets for Molecular Calculations*; Elsevier: Amsterdam, 1984; p 16.
(37) Dunning, T. H., Jr.; Hay, P. J. In *Modern Theoretical Chemistry*; Schaefer, H. F., III, Ed.; Plenum Press: New York, 1977; Vol. 3, pp 1−28.

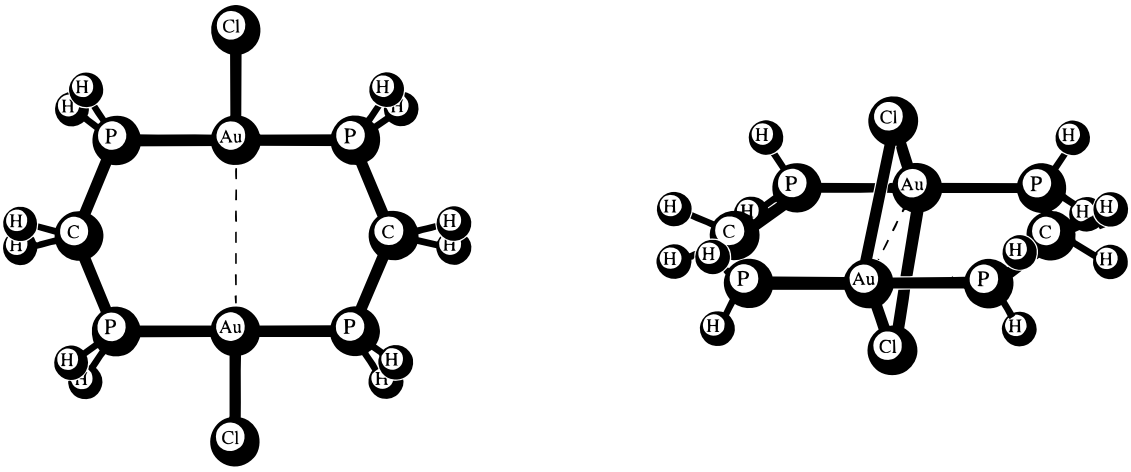

Figure 3. Cl atoms in molecular plane and in bridging positions in $[Au(PH_2CH_2PH_2)]_2Cl_2$.

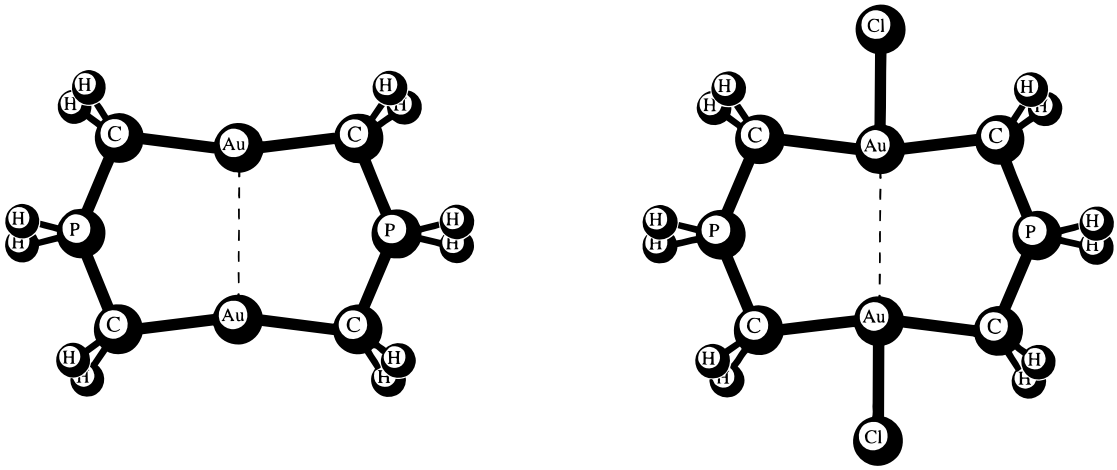

Figure 4. Models of eight-membered rings with a d^9-d^9 $Au^{II}-Au^{II}$ bond.

Table 1. Basis Sets and Pseudopotentials (PP) Used in the Present Work

atom	PP	basis	remarks
H	−	(4s1p)/[2s1p]	$\alpha_p = 0.8$[37]
C	Bergner[35]	(4s4p1d)/[2s2p1d]	$\alpha_p = 0.1561$, $\alpha_d = 0.80$
N	Bergner[35]	(4s4p1d)/[2s2p1d]	$\alpha_p = 0.222$, $\alpha_d = 0.864$
P	Bergner[35]	(4s4p1d)/[2s2p1d]	$\alpha_p = 0.084$, $\alpha_d = 0.34$
S	Bergner[35]	(4s4p1d)/[2s2p1d]	$\alpha_p = 0.1017$, $\alpha_d = 0.4210$
F	Bergner[35]	(4s4p1d)/[2s2p1d]	$\alpha_p = 0.0848$, $\alpha_d = 1.496$
Cl	Bergner[35]	(4s4p1d)/[2s2p1d]	$\alpha_p = 0.0154$, $\alpha_d = 0.514$
Br	Bergner[35]	(4s4p1d)/[2s2p1d]	$\alpha_p = 0.0361$, $\alpha_d = 0.389$
I	Bergner[35]	(4s4p1d)/[2s2p1d]	$\alpha_p = 0.0326$, $\alpha_d = 0.266$
Te	Bergner[35]	(4s4p1d)/[2s2p1d]	$\alpha_p = 0.029767$, $\alpha_d = 0.237$
Au	Andrae[32]	(8s6p5d1f)/[6s5p3d1f]	$\alpha_f = 0.2$
Au	Andrae[32]	(8s6p5d2f)/[6s5p3d2f]	$\alpha_f = 0.2, 1.19$
Au	11-VE LANL1DZ[33]	LANL1DZ basis for Au	$\alpha_f = 0.20$
Ag	Andrae[32]	(8s6p5d1f)/[6s5p3d1f]	$\alpha_f = 0.22$
Ag	Andrae[32]	(8s6p5d2f)/[6s5p3d2f]	$\alpha_f = 0.22, 1.72$
Cu	Dolg[34]	(8s6p5d1f)/[6s5p3d1f]	$\alpha_f = 0.24$
Cu	Dolg[34]	(8s6p5d2f)/[6s5p3d2f]	$\alpha_f = 0.24, 3.70$

(i) $[(M^I)_2(PH_2CH_2PH_2)_2]^{2+}$ and $[(Au^I)_2(PH_2CH_2PH_2)_2]Cl_2$ Systems. The calculations without the Cl counterions could be performed at the best level (19 VE PP, 2f) and are reported in Table 2. The systems with counterions were treated at the 1f level. The effects of the counterions and the (11 VE/19-VE) pseudopotential are reported in Table 3.

In the $[Au_2(PH_2CH_2PH_2)_2]^{2+}$ model system (see Figure 1), the calculated P−Au and Au−Au bond lengths, and the PAuP angle are close to experiment when we have used the 19-VE Andrae PP and a 1f basis at MP2 level. The Au−Au distance is reduced by 12 pm, if a 2f basis is employed. When we used the 11-VE LANL1DZ PP, the covalent Au−P bond lengths and the free-cation Au−Au distance is too short. Similar trends were found for the $[XAuPH_3]_2$ case in Part I.[7] Our obtained geometries for the $[Au_2(PH_2CH_2PH_2)_2]^{2+}$ model are different from those reported by A. Laguna and co-workers.[24] We do not know why their results differ from ours.

In numerous solid compounds with eight-membered dications, the anions, X^-, lie along the $X^-{-}Au{-}Au{-}X^-$ axis. When they are explicitly included in the calculation, little change is

Table 2. Optimized Geometries for the $[M_2(PH_2CH_2PH_2)_2]$ at MP2 and HF 2f Levels (Distances in pm and Angles in deg)

system	method	PP	M−M	P−M	P−C	P−M−P	P−C−P	P···P
$[Au_2(PH_2CH_2PH_2)_2]^{2+}$	MP2	19-VE	284.2	234.1	187.1	171.3	117.4	319.6
	HF	19-VE	319.0	243.2	187.4	178.4	120.7	325.7
$[Ag_2(PH_2CH_2PH_2)_2]^{2+}$	MP2	19-VE	283.9	239.9	187.5	171.8	116.1	318.1
	HF	19-VE	315.9	261.6	188.1	178.3	118.6	317.9
$[Cu_2(PH_2CH_2PH_2)_2]^{2+}$	MP2	19-VE	284.3	220.0	187.2	171.2	116.2	317.9
	HF	19-VE	311.8	238.0	187.5	177.2	119.4	323.6

Table 3. Optimized Geometries for the $[M_2(PH_2CH_2PH_2)_2]$ at MP2 and HF Levels (Distances in pm and Angles in deg; Results with 1f Orbital on Metallic Center)

system	method	PP	M−M	P−M	M−Cl	P−C	P−M−P	P−C−P	P···P
$[Au_2(PH_2CH_2PH_2)_2]^{2+}$	MP2	19-VE	296.9	234.1	−	185.9	174.5	118.5	319.5
	HF	19-VE	312.7	244.8	−	187.8	177.3	119.3	324.0
$[Au_2(PH_2CH_2PH_2)_2]^{2+}$	MP2	11-VE	287.5	246.1	−	186.6	172.6	117.6	319.3
	HF	11-VE	309.2	248.1	−	187.2	176.7	119.5	323.4
$[Ag_2(PH_2CH_2PH_2)_2]^{2+}$	MP2	19-VE	293.4	243.1	−	187.6	173.7	116.9	319.9
	HF	19-VE	310.7	261.7	−	187.9	177.3	118.4	322.9
$[Au_2(PH_2CH_2PH_2)_2]Cl_2$ [a]	MP2	19-VE	296.2	235.4	260.4	187.8	175.6	113.7	314.5
	HF	19-VE	316.3	247.7	271.3	188.1	179.4	115.9	318.9
$[Au_2(PH_2CH_2PH_2)_2]Cl_2$ [b]	MP2	19-VE	289.1	232.9	278.4	188.2	171.5	118.5	323.5
	HF	19-VE	313.1	243.3	306.3	188.0	176.9	120.4	326.4

[a] Cl atoms in molecular plane. [b] Bridging Cl atoms.

Table 4. Selected Experimental Structural Parameters[a] for $[M_2(XZX)_2]$ (Distances in pm and Angles in deg; Type of the Prototype Ligand, L, Is Given in the First Column)

L	compound	M−M	X−M	M−Cl	X−Z	X−M−X	X···X	ref
1	$[Cu_2(form)_2]$[b]	249.7	188.6	−	127.6	185.5	245.6	17
	$[Ag_2(form)_2]$[b]	270.5	211.6	−	128.9	191.2	250.5	17
2	$[Au_2(Et_2NCS_2)_2]$	276.1	228.2	−	170.0	180	305.0	18
3	$[Ag(dppm)(NO_3)]_2$ [c]	308.5	242.6		182.5	138.3		19
	$[Au_2(\mu\text{-dmpm})_2]Cl_2$ [d]	301.4	230.2	350.5	181.3	176.8	308.4	20
	$[Au_2(dppm)_2]Cl_2$ [e]	296.2	232.7	277.1	183.0	155.9	307.2	21
	$[Au_2(cdpp)_2]Cl^+$ [f]	290.7	231.2	280.7	183.7	171.5	306.3	21

[a] All structures were obtained by from X-ray diffraction. [b] Form = (MePh)NCHN(MePh). [c] dppm = $H_2C(PPh_2)_2$. Average values given. [d] dmpm = $CH_2(PMe_2)_2$. Bridging Cl atoms. [e] Cl atoms in molecular plane. [f] cdpp = $(CH_2)_2C(PPh_2)_2$. Bridging Cl atom.

Table 5. Optimized Geometries for the $[M_2(NHCHNH)_2]$ at MP2 and HF Levels (Distances in pm and Angles in degr; 19-VE PP for the Metal Atoms)

system	method	f	M−M	N−M	N−C	N−M−N	N−C−N	N···N
$[Au_2(NHCHNH)_2]$	MP2	2	272.8	200.5	132.4	190.5	126.1	235.9
	HF	2	289.2	208.7	130.3	195.3	127.3	233.5
$[Ag_2(NHCHNH)_2]$	MP2	2	271.2	204.3	132.2	190.1	125.4	235.0
	HF	2	286.7	217.1	130.3	194.3	126.3	232.6
$[Cu_2(NHCHNH)_2]$	MP2	2	252.8	183.4	132.2	186.1	123.7	233.1
	HF	2	262.8	193.2	130.2	189.4	125.2	231.1

observed in the ring geometry, see Table 3. Larger changes are observed in the halogen-bridged case.

The Cl^- anions form an ionic bond with gold atoms, and hence the changes in the structure of the ring remain small. The bridging structure is 66.8 kJ/mol more stable than the planar one for the 19-VE PP. This tendency is in agreement with the experimental results.[20]

The transannular Au^I-Au^I distance in different models containing gold (Tables 2 and 3) shows a reduction between 15 and 35 pm from HF to MP2 level. We therefore conclude that a metallophilic attraction is present. Further evidence is given by the PAuP angle, which is reduced by several degrees.

The calculated Au−Au distance at the 19VE 1f MP2 level, 297 pm, is close to the experimental values for **3** in Table 4. The Au−Au distance at the 2f level, 284 pm is shorter than experiment. As found in Part I,[7] the MP2 method and 88.5 kJ/mol for 11-VE LANL1DZ PP exaggerates the V(Au−Au). At the 1f level the basis-set error and the errors of the MP2 method may cancel.

The hypothetical model system containing copper was also considered, the results are shown in Table 2. The transannular M^I-M^I distance and PMP angles again show a reduction from HF to MP2 level.

(ii) $[M_2(NHCHNH)_2]$ Systems. The optimized 1f and 2f geometries for these systems are given in Table 5. For this model, we have found a reduction between 15 and 8 pm in the M^I-M^I distances from HF to MP2 level. The results using 1f or 2f basis sets are closely similar.

The results for the models containing silver and copper are close to the experimental structures of $[M_2(form)_2]$ (see Tables 4 and 5).[17] Here "form" stands for (MePh)N(CH)N(MePh). For instance, the Cu−Cu distance is 249.7 and 251.8 pm at the experimental and theoretical level, while the NCuN angle is 185.5 and 186.5°, respectively. The same is true for the silver model. Although the M−M distance exceeds the N−N one, indicating M−M repulsion ($R < R_e$, $\alpha > 180°$), correlation effects still shorten the M−M distance. Romero and co-workers have studied the $Ag_2(NHCHNH)_2$ system at SCF level (without f functions) and used a LANL2DZ PP.[38] They have obtained

(38) Romero, M. A.; Salas, J. M.; Quiros, M.; Sánchez, M. P.; Molina, J.; Bahraoui, J. E.; Faure, R. *J. Mol. Struct.* **1995**, *354*, 189.

Table 6. Optimized Geometries for the $[M_2(SCHS)_2]$ at MP2 and HF Levels (Distances in pm and Angles in deg; 19-VE PP for Each Metal)

system	method	f	M−M	S−M	S−C	S−M−S	S−C−S	S···S
$[Au_2(SCHS)_2]$	MP2	2	282.4	230.3	168.1	172.5	136.7	312.5
	HF	2	300.6	240.5	167.2	177.6	134.7	310.7
$[Ag_2(SCHS)_2]$	MP2	2	278.5	234.1	168.0	171.9	136.0	311.6
	HF	2	300.9	251.4	167.3	178.2	134.7	308.9
$[Cu_2(SCHS)_2]$	MP2	2	272.6	214.6	167.7	170.3	131.9	306.5
	HF	2	287.1	229.1	167.3	174.8	134.0	307.9

Table 7. Optimized Geometries for the $[Au(CH_2PH_2CH_2)]_2$ at MP2 Level (Distances in pm and Angles in deg; 19-VE PP for Each Metal)

system	f	method	Au−Au	C−Au	Au−Cl	C−P	C−Au−C	C−P−C
$[Au(CH_2PH_2CH_2)]_2$	1	MP2	292.4	208.8	−	180.9	173.1	122.73
$[Au(CH_2PH_2CH_2)]_2Cl_2$ [a]	1	MP2	260.9	209.7	238.8	178.1	168.9	115.59
$[Au(CH_2PH_2CH_2)]_2^{2+}$	1	MP2	283.4	209.9	−	185.9	164.4	132.5
$[Au(CH_2PPh_2CH_2)]_2$	−	expt[b]	297.7	209.1	−	176.0	179.0	113.0
$[Au(CH_2P(CMe)_2CH_2)]_2Cl_2$ [a]	−	expt[c]	259.7	194.2	235.9	187.9	−	−

[a] Cl atoms in molecular plane. [b] Reference 41. [c] Reference 40.

Table 8. NBO Analysis in $[Au(CH_2PH_2CH_2)]_2$ and $[Au(CH_2PH_2CH_2)]_2Cl_2$ at MP2 Level

system	atom	natural charge	natural electron configuration
$[Au(CH_2PH_2CH_2)]_2$	Au	0.309	6s(0.98)5d(9.58)6p(0.05)7s(0.01)5f(0.03)6d(0.05)7p(0.01)
	P	1.188	3s(1.10)3p(2.62)3d(0.08)4p(0.02)
	C	−1.213	2s(1.27)2p(3.88)3s(0.01)3p(0.04)3d(0.02)
	H(P)	−0.021	1s(1.01)2p(0.01)
	H(C)	0.243	1s(0.75)2p(0.01)
$[Au(CH_2PH_2CH_2)]_2Cl_2$	Au	0.682	6s(0.79)5d(9.34)6p(0.09)7s(0.01)5f(0.04)6d(0.06)7p(0.01)
	P	1.197	3s(1.09)3p(2.62)3d(0.08)4p(0.01)
	C	−1.156	2s(1.26)2p(3.83)3s(0.01)3p(0.04)3d(0.02)
	Cl	−0.604	3s(1.96)3p(5.55)3d(0.07)4p(0.02)
	H(P)	−0.008	1s(1.00)2p(0.01)
	H(C)	0.263	1s(0.73)2p(0.01)

an Ag−Ag distance of 292.5 pm and NAgN angle of 194.7°. These values are comparable with our calculations at the HF level.

The hypothetical gold compound would have an Au−Au distance at the MP2 level of 274 pm, a typical value for the experimentally known, doubly bridged Au(I) systems.

(iii) $[M_2(SCHS)_2]$ Systems. The optimized geometries for these models are given in Table 6. The M^I-M^I distances and SMS angles are reduced from HF to MP2 level, while the structure of the ligand remains almost constant.

When we employ a 2f basis set on the metal, at MP2 level a reduction of about 8 pm in M^I-M^I distances and 3° in SMS angles is found. At HF level, there are no differences between the 1f and 2f geometries.

The results for gold models are close to experimental ones (see Table 4).[18] For instance, the Au−Au distance is 276 and 282.4 pm, at experimental and theoretical level, respectively. However, the SAuS angle is 180 and 172.5°, for experiment and theory, respectively. It should be emphasized that this experimental structure of $[Au_2(Et_2NCS_2)_2]$ is twisted.[18]

In general, for these eight-membered rings, the intramolecular M^I-M^I theoretical contacts are comparable in magnitude to experimental results, provided that electronic correlation, at MP2 level, is included. The structures of the bridging XZX ligands are well reproduced at both HF and MP2 levels. This is a clear evidence for an intramolecular, correlation-induced attraction in these three types of rings.

B. Oxidized Eight-Membered Rings. In order to underline the difference between the Au(I)−Au(I) interaction and the (formally d^9-d^9) $Au^{II}-Au^{II}$ bond,[39] we consider two examples of the latter. They are $[Au(CH_2PH_2CH_2)]_2^{2+}$ and $[Au(CH_2PH_2CH_2)]_2Cl_2$ (see Figure 4); in the latter case the counterions are explicitly included.

The optimized geometries are given in Table 7, together with experimental results.[40,41] When the neutral $[Au(CH_2PH_2CH_2)]_2$ is oxidized by including two Cl atoms, the MP2 1f Au−Au distance drops from 292 to 261 pm and the C−Au−C angle from 173 to 169°. A calculation on the oversimplified $[Au(CH_2PH_2CH_2)]_2^{2+}$ model yields a too long Au−Au distance of 283.4 pm and a C−Au−C angle of 164.4°.

The results of natural bond orbital (NBO) analyses of the MP2 densities are given in Table 8. The Au(I) and Au(II) have charges of +0.31 and +0.68, respectively. The removal of 0.37 electrons from each gold atom occurs about equally from the 6s and the 5d shells. Note the 6s population of both the Au(I) and the Au(II) compound, $6s^{0.79}$ for the latter. Hence the $Au^{II}-Au^{II}$ bond is definitely not a pure $d\sigma-d\sigma$ one. The Au 6s span the A_g and B_{2u} irreps. Note the strong stabilization of the lower A_g.

The orbitals accounting for the oxidative addition of chlorine are schematically shown in Figure 5. The two Cl ligands produce A_g and B_{2u} combinations, which interact strongly with HOMO B_{2u} and the A_g orbitals of the unoxidized complex. The Au−Au interaction is increased by electron transfer out of the B_{2u} MO of the neutral $[Au(CH_2PH_2CH_2)]_2$ to the chlorines. The A_g HOMO consists largely of Cl orbitals. The lower A_g is strongly stabilized. The present ab initio analysis fully supports the model proposed by Hoffmann et al.[42] for the $Au^{II}-Au^{II}$ interaction.

C. Di-μ-halogenodihalogenometal(I) Systems. We have fully optimized the geometries for $[M_2X_4]^{2-}$ (M = Cu, Ag, Au; X = Cl, Br, I) at HF and MP2 levels (see Figure 2). A D_{2h}

(39) Fackler, J. P., Jr. *Polyhedron* **1997**, *16*, 1.

(40) Schmidbaur, H.; Mandl, J. R.; Frank, A.; Huttner, G. *Chem. Ber.* **1976**, *109*, 466.

(41) Basil, J. D.; Murray, H. H.; Fackler, J. P.; Tocher, J.; Mazany, A. M.; Trzcinska-Bancroft, B.; Knachel, H.; Dudis, D.; Delord, T. J.; Marler, D. O. *J. Am. Chem. Soc.* **1985**, *107*, 6908.

(42) Jiang, Y.; Alvarez, S.; Hoffmann, R. *Inorg. Chem.* **1985**, *34*, 426.

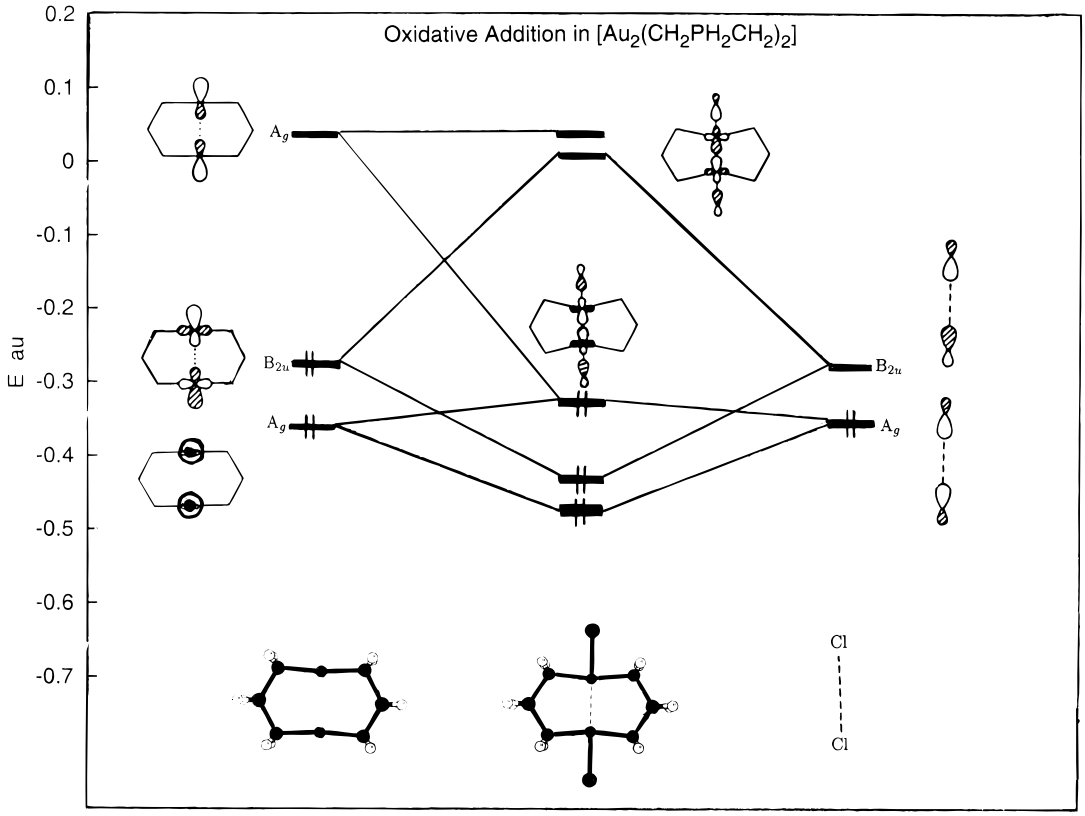

Figure 5. Partial interaction diagram for oxidative addition of Cl_2 to $[Au(CH_2PH_2CH_2)]_2$. HF orbital energies are given.

Table 9. Optimized Geometries for the $[M_2X_4]^{2-}$ at HF and MP2 Levels (Distances in pm and Angles in deg; 19-VE PP and 2f Basis for Each Metal)

system	method	M−X_t	M−X_b	M−M	M−X_b−M	X_b−M−X_b	X_b−M−X_t	X_b−X_b
$[Au_2Cl_4]^{2-}$	MP2	234.8	254.9	385.0	98.10	81.89	139.1	334.1
	HF	249.8	274.4	402.9	94.48	85.51	137.2	372.6
$[Ag_2Cl_4]^{2-}$	MP2	243.9	253.9	316.7	77.17	102.8	128.6	396.9
	HF	259.9	275.0	380.1	87.43	92.56	133.7	397.5
$[Cu_2Cl_4]^{2-}$	MP2	218.6	232.4	314.1	85.02	94.98	132.5	342.7
	HF	236.6	250.8	337.7	84.62	95.38	132.3	370.9
$[Au_2Br_4]^{2-}$	MP2	246.9	264.9	388.9	94.44	85.55	137.2	359.9
	HF	262.2	285.6	408.9	91.40	88.59	135.7	399.0
$[Ag_2Br_4]^{2-}$	MP2	256.3	264.5	291.5	66.87	113.1	146.5	441.4
	HF	273.1	287.7	389.4	85.20	94.79	132.6	423.5
$[Cu_2Br_4]^{2-}$	MP2	234.8	241.9	262.0	65.58	114.4	122.8	406.7
	HF	250.5	263.8	346.0	81.96	98.04	130.9	398.4
$[Au_2I_4]^{2-}$	MP2	268.3	282.1	264.6	55.94	124.1	117.9	498.3
	HF[a]	–	–	–	–	–	–	–
$[Ag_2I_4]^{2-}$	MP2	273.2	279.3	284.6	61.25	118.7	120.6	480.6
	HF	291.3	305.7	402.6	82.39	97.60	131.2	459.9
$[Cu_2I_4]^{2-}$	MP2	254.9	258.2	248.1	57.43	122.6	118.7	452.8
	HF	270.6	283.6	362.8	79.53	100.5	129.8	436.0

[a] No minimum found.

Table 10. Selected Experimental Structural Parameters[a] for $Y_2[M_2X_4]$ (Distances in pm and Angles in deg)

system	M−X_t	M−X_b	M−M	M−X_b−M	X_b−M−X_b	X_b−M−X_t	X_b−X_b	ref
$[As(C_6H_5)_4]_2[Ag_2Cl_4]$	235.9	244.6	365.9	87.97	92.03	149.06	378.9	29
$[P(C_6H_5)_4]_2[Cu_2Cl_4]$	211.2	213.5	351.6	86.59	93.42	165.77	372.2	29
$[P(C_6H_5)_4]_2[Ag_2Br_4]$	249.1	261.7	357.8	83.53	96.47	140.38	400.6	29
$(TTT)_2[Cu_2Br_4]$	232.8	247.2	266.0	64.70	115.4	125.0	–	29
[K(crypt-2,2,2)]$_2[Ag_2I_4]$	267.2	278.9	355.7	79.02	100.98	127.65	431.3	29
$[As(C_6H_5)_4]_2[Cu_2I_4]$	249.0	257.8	266.3	61.40	111.2	120.9	436.0	29

[a] All structures were obtained by from X-ray diffraction.

symmetry was assumed. The results are given in the Table 9 for a 2f basis sets at each metallic center. For some silver and copper systems, experimental crystallographic results are given in Table 10.

The copper results in Figure 6a at HF level show a systematic decrease of the Cu−X_b−Cu angle along X = Cl, Br, I, corresponding to the larger size of the X atom. At the MP2 level (1f or 2f), the X = Cl results are very similar and all the

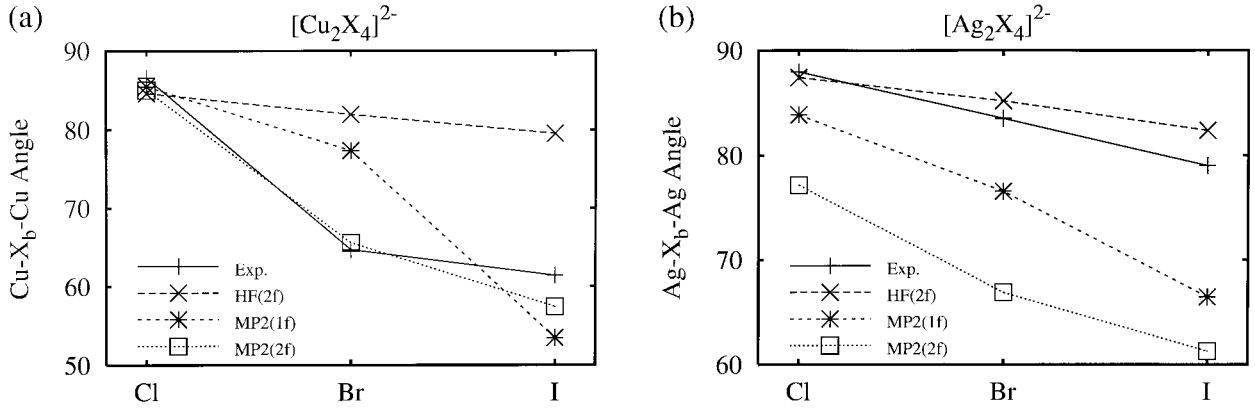

Figure 6. Calculated and experimental M−X_b−M angles of the $[M_2X_4]^{2-}$ species as function of the halogen, X; (a) M = Cu, (b) M = Ag.

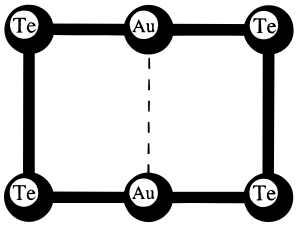

Figure 7. $[Au_2Te_4]^{2-}$ system.

calculations are close to experiment. For X = Br and I, the experimental angle drastically drops to 65° or below. The MP2 curves follow the same trend. All this could be explained as M···M metallophilic attraction becoming the dominant structural principle for M = Cu and X = Br, I. The MP2 Cu−Cu distances of 262 and 248 pm, respectively, fall in the metallophilic range for copper (see Table 7 of reference 3).

The M = Ag trends in Figure 6b are similar to those for M = Cu at the HF level, but now the experimental angles show a systematic decrease that is only slightly faster than the HF one. The collapse to the predicted narrow-angle structure doesn't take place in the two experimental $[Ag_2Br_4]^{2-}$ and one $[Ag_2I_4]^{2-}$ structures listed by Jagner and Helgesson (see Table III of reference 29). Short Ag−Ag distances, however, occur in $[AgX_2]$ chains (see Table VI of reference 29).

For the hypothetical $[Au_2X_4]^{2-}$ gold systems, the X = Cl, Br ligands leave the Au−Au distance long while X = I gives a very short Au−Au distance of 265 pm and a small Au−I_b−Au angle of 56° at MP2 level.

The present results thus suggest an interesting bistability of the M−X_b−M angle and the M−M distance. The agreement with experiment and the very large HF−MP2 changes indeed suggest that the M−M attraction is the driving force behind the narrow M−X_b−M angles, although results for a flexible dianion, with no provision for the counterions in the crystal, should be treated with caution. As discussed in the reviews 3 (see Table 10 therein) and 43, an analogous bistability occurs in the solid AuX monohalides. They have chain structures. The chloride has an Au−X−Au angle of 92°, the iodide 72.6°, and the bromide occurs in two modifications with an angle of 92.3 or 77°.

D. $[Au_2Te_4]^{2-}$ System. We have fully optimized the geometry for $[Au_2Te_4]^{2-}$ (Figure 7) at the HF and MP2 levels. A D_{2h} point symmetry was assumed. The results are given in Table 11, together with experimental results.[16]

The Au^I−Au^I distance shows a dramatic reduction of 39 pm from HF to MP2 level. Use of a second polarization f function on gold made no difference. In this case electron correlation effects also shorten the Au−Te distance by 16 pm. The Au−Te distance is close to the experimental value, the calculated Au−Au one is much too small. While a free-ion calculation on a dianion without any counterion stabilization is approximate at best, the shortening of the Au−Au distance is interesting. Note also that the MP2 level exaggerates the aurophilic attraction.[7]

Table 11. Optimized Geometries for the $[Au_2Te_4]^{2-}$ at HF and MP2 2f Levels (Distances in pm and Angles in deg; 19-VE PP for Each Metal)

system	method	Au−Au	Au−Te	Te−Te	Te−Au−Au
$[Au_2Te_4](TPP)_2$	exptl[a]	296.0	254.0	272.0	87.6
$[Au_2Te_4]^{2-}$	MP2	279.3	257.9	287.9	90.96
	HF	318.5	273.1	283.1	86.28

[a] Reference 16. TPP = tetraphenylphosphonium.

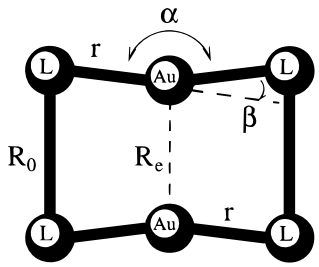

Figure 8. Simple mechanical model for L−Au−L bending due to the intra-ring Au−Au interaction.

The calculated Au−Te bond length of 258 pm can be compared with that of 254 pm found in $(TPP)_2[Au_2Te_4]$. The length of a single Te−Te bond is typically 271 pm,[44] close to the present one. Note that the Te−Au−Te axes are bent outward in the crystal and inward at MP2 level.

E. Mechanical Model. Since the earliest structural studies, the presence of an Au−Au attraction was deduced from a bending of one X−Au−Y system toward its neighbor. The internal consistency of this idea can actually be checked by calculating first the bending force constant of one monomer, and the potential, $V(R)$, of the attraction.

In the simple model shown in Figure 8 the distance between the ligand atoms, L−L, or R_0, and the M−L distance, r, are fixed. The forces resulting from the metal−metal interaction are here expressed by the four-parameter fit

$$V_M = Ae^{-BR} - CR^{-n} \quad (1)$$

(43) Jones, P. G. *Gold Bull.* **1981**, *14*, 102.

(44) Klinkhammer, K. W.; Pyykkö, P. *Inorg. Chem.* **1995**, *34*, 4134.

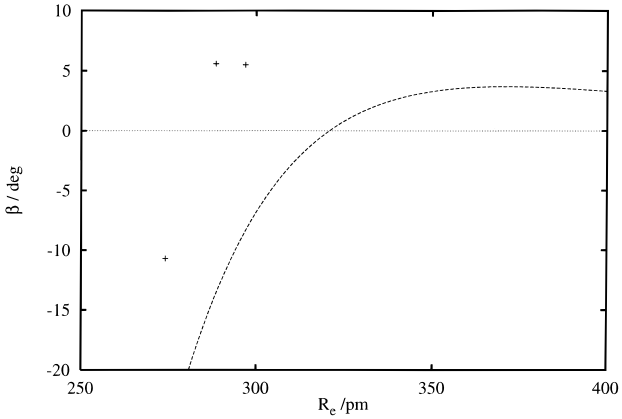

Figure 9. Bending angle $\beta = 180° - \alpha$ as function of the Au−Au distance, R_e. The curve (- - -) is given by eq 3 with parameters for the perpendicular 19-VE 2f free dimer $(ClAuPH_3)_2$. The points (+) are from the present calculations for eight-membered ring systems.

where R is the M−M distance. The combined bending potential of the two monomers is expressed as

$$V_b(\beta) = k_\beta \beta^2 \qquad (2)$$

At equilibrium, $R = R_e$, the two forces dV/dR are assumed to cancel. Here, $\beta = 180° - \alpha$ (see Figure 8); a shorter Au−Au distance implies a more positive β, thus if $R_e < R_0$, $\beta > 0$ and if $R_e > R_0$, $\beta < 0$. When R_0 is held constant, the intramonomer L−L distance will change slightly. Then to first order in β^2, at the equilibrium M−M distance, R_e:

$$(\beta/\mathrm{deg}) = \frac{\pi}{360 k_\beta} r[AB\mathrm{e}^{-BR_e} - CnR_e^{-(n+1)}] \qquad (3)$$

Using the typical values (for perpendicular $(ClAuPH_3)_2$ dimers, from Part I,[7] $A = 126.62$ au, $B = 0.02997$ pm^{-1}, $C = 4.1198 \times 10^9$ Hartree pm^n, $r = 234$ pm, $n = 4.53309$), and the typical bending force constant $k_\beta = 3.1644 \times 10^{-5}$ Hartree/deg^2, one obtains the behavior in Figure 9. It is seen that the maximum inward bending of about 3° occurs around $R_e = 360$ pm.

The calculated points for the present systems agree qualitatively with the predicted curve, verifying that the observed bending of the monomers can in principle be attributed to the metallophilic attraction. The present doubly bridged rings with soft ligands, L, have shorter R_e and probably stronger interactions than the unbridged $(ClAuPH_3)_2$ model. The model could be improved by introducing an L−L force constant, k_{LL}.

IV. Conclusions

The present comparison of HF and MP2 calculations demonstrates again the importance of correlation effects in shortening the M^I-M^I distance. We have now considered this effect in doubly bridged ring systems. More specifically,

(1) The 19-VE 1f MP2 geometry of $[Au_2(PH_2CH_2PH_2)_2]^{2+}$ is close to experiment. The 2f (two f functions on Au) MP2 Au−Au distance is too short. Thus good results for intramolecular geometries at the 1f MP2 level may depend to some extent on error compensation between MP2 overestimation and 1f underestimation of the Au−Au interaction.

(2) The thioformiate Au−Au distances are slightly above experiment at both the 1f and 2f level.

(3) For the hard, small-bite ligand NHCHNH, the calculated Cu−Cu distance of 253 pm is clearly shorter than the Ag−Ag one of 271 pm. Both are close to experiment. While very long Cu−Cu distances, comparable with the Ag−Ag and Au−Au ones, were found for perpendicular, free $[ClCuPH_3]_2$ dimers,[7] this ring has short ones.

(4) For this "small-bite" ligand, a metallophilic attraction, as estimated by the HF to MP2 difference, causes a shortening of the Cu−Cu distance of about 10 pm.

(5) When the Au(I) in $[Au_2(CH_2PH_2CH_2)_2]$ model are oxidized to Au(II) by Cl_2, the Au−Au distance is shortened to 261 pm, in agreement with experiment. The shortening is attributed to a σ bond between gold(II) atoms. Although nominally $5d^9$, these gold atoms have substantial 6s populations.

(6) The short M−M distances and sharp $M-X_b-M$ angles in $Cu_2Br_4^{2-}$ and $Cu_2I_4^{2-}$ may be attributed to the "metallophilic" attraction.

Acknowledgment. P.P. thanks The Academy of Finland (FA) for a Research Professorship in August 1995−July 2000. F.M. also is supported by FA. Both the Dec AlphaStations of this Laboratory and computer resources from Center for Scientific Computing (CSC), Espoo, were used.

IC980121O